Modeling of Polymer Crystallization in Plates, Pipes, and Rods During Cooling

Ewa Piorkowska, Andrzej Galeski

Centre of Molecular and Macromolecular Studies, Polish Academy of Sciences, 90 363 Lodz, Sienkiewicza 112, Poland

Received 25 April 2001; accepted 2 April 2002

ABSTRACT: We modeled crystallization of isotactic polypropylene inside plates, rods, and pipes during cooling. The modeling was based on the solution of the heat conduction equation, which takes into account the liberation of the heat of crystallization. The predictions of polymer crystallization kinetics was based on differential scanning calorimetry data and on spherulite growth rate measurements. The influence of size on the crystallization process was determined. © 2002 Wiley Periodicals, Inc. J Appl Polym Sci 86: 1363–1372, 2002

Key words: crystallization; isotactic poly(propylene) (iPP)

INTRODUCTION

Crystallization is accompanied by release of the latent heat of fusion. Hence, the initial temperature distribution changes inside a material undergoing solidification. In metals and other low-molecular substances, an interphace, at which the transformation occurs, follows an isotherm of the melting point. The process of transformation is then controlled by heat dissipation. Polymer crystallization usually proceeds at large supercoolings, well below the melting point because it is controlled by primary and secondary nucleation rather than by the dissipation of the latent heat of fusion. After the primary nucleation, a crystalline aggregate, a spherulite, grows until impingement with neighboring spherulites. The temperature near the crystallization front might be increased by the liberation of the latent heat of fusion but may still be well below the melting temperature of the crystals. Polymers are poor heat conductors, hence, except for thin films, the temperature increases during crystallization in bulk.[1–7] The temperature increase in a polymer due to crystallization either during cooling[3–7] or at isothermal ambient conditions[1] has been experimentally measured. The cooling of thick wall products during industrial processes results in significant temperature gradients that are enhanced by the liberation of the heat of crystallization. The crystallization inside a material occurs at an elevated temperature, which is unfavorable for the strength and toughness of a polymer. Therefore, it is important to have the ability to predict both the course of crystallization and the temperature inside thick-walled products during cooling from a molten state in industrial processing conditions.

The conversion of melt into spherulites was first described by Evans[8] and Avrami.[9] An earlier approach to the problem by Kolmogoroff[10] was inaccurate: errors made in his derivation canceled themselves, leading accidentally to the correct result (see Appendix). Nevertheless, the final equation for the conversion degree, equivalent to that obtained by Avrami for isothermal crystallization, was successfully used to describe the overall kinetics of crystallization.[11] To apply the Avrami and Evans theory, knowledge of the spherulite nucleation rate and the growth rate for the chosen polymer is required. Because nucleation is mainly heterogeneous at low and moderate undercoolings, it is controlled by impurities in a polymer, both accidental or introduced on purpose. Although the growth rate depends on temperature, the nucleation of spherulites depends also on time, and it is influenced by the thermal history of the polymer. Therefore, the application of nucleation data obtained from isothermal experiments to the prediction of nonisothermal processes is limited. During crystallization in bulk, the liberation of the heat of fusion, dependent on the conversion rate, modifies the temperature field resulting from cooling. Therefore, the modeling of the solidification in bulk involves solving the heat conduction equation, which accounts for the heat production inside a polymer related to the nucleation and growth of spherulites.

In uniform temperature field, spherulite growth occurs in radial directions, whereas a temperature gra-

Correspondence to: E. Piorkowska (epiorkow@bilbo.cbmm.lodz.pl).

Contract grant sponsor: Polard State Committee for Scientific Research through the Centre for Molecular and Macromolecular Studies, Polish Academy of Sciences; contract grant number: 7 T08 016 12.

dient results in anisotropy of spherulite growth and shapes and also in changes in growth trajectories.[12,13] Therefore, to account for the detailed effects of the temperature gradient on spherulite growth and morphology, computer simulation of spherulitic growth is necessary. Recently, the solidification of polyethylene in a mold was computer simulated,[14,15] on the basis of the tracking of two-dimensional spherulite growth in a variable temperature field. The influence of a constant temperature gradient on the spherulite pattern and the conversion of melt into spherulites in isotactic polypropylene (iPP) film was evaluated by means of computer simulation and also by the probabilistic model by Piorkowska.[16] The simulation of spherulitic growth in a temperature field in bulk would require, however, the tracking of the three-dimensional growth fronts of a large number of spherulites, which is far more complicated than the use of analytical expressions for the conversion rate in nonisothermal conditions.

In the past, the temperature and the conversion of melt into spherulites were modeled inside 2 mm thick iPP plates solidified at a constant ambient temperature.[1] The solidification of iPP in quenched slabs was modeled in refs. [3] and [4]. In ref. [4], the conversion of melt into spherulites during nonisothermal crystallization was described with the help of the equation derived by Nakamura[17] for isokinetic conditions when the parameters used to describe the nucleation (e.g., nucleation rate) depend on the temperature in the same way as the spherulite growth rate and when it is possible to predict the conversion on the basis of isothermal experiments data. However, the nucleation process depends not only on the momentary temperature but also on the thermal history of a polymer, for example, cooling rate, and therefore, the isokinetic models have limited application, especially if the cooling is fast.

The present article is devoted to modeling iPP crystallization in pipes, rods, and plates during cooling. The temperature distribution and the progression of crystallization inside such objects during the entire cooling process were calculated. The applied procedure was similar to that described earlier in ref. [1] for the solidification in iPP plates in ambient isothermal conditions. The solution of the heat conduction equation, which accounts for the heat production rate dependent on time and position, was used and combined with the analytical expression for conversion rate during a nonisothermal crystallization. The influence of the size and shape of crystallizing objects on the temperature decline and on the progression of crystallization was evaluated. The experimental data on spherulite growth rate and nucleation were applied for the prediction of crystallization inside the considered objects as dependent on cooling rate and momentary local temperature. The spherulite growth rate temperature dependence was measured, and the nonisothermal crystallization during cooling at various rates was studied by means of differential scanning calorimetry (DSC) for selected iPP. The temperature field was modeled with the help of the heat conduction equation in the form proper for the geometry of the considered article, which accounted for the heat production due to crystallization. The temperature decline inside an iPP plate was measured during cooling and compared with the theoretical predictions.

MODELING OF HEAT TRANSPORT

The heat transport in a plate of length and width large as compared with its thickness (d) can be described by the equation:

$$\frac{\delta^2 T}{\delta x^2} - a^{-1}\frac{\delta T}{\delta t} = K^{-1}A(x,t) \tag{1}$$

where T, t, and x are the temperature, time, and distance from one of the surfaces; $A(x,t)$ is the rate of heat production rate per unit volume; and K and a denote the heat conductivity and thermal diffusivity of the polymer, respectively.

It is assumed that the plate is initially at a constant temperature: $T(0,x) = T_0$. The temperature of the surfaces is suddenly changed and kept at constant level (T_e): $T(t,0) = T(\mathrm{t},d) = T_e$. However, the heat transfer at the boundary of the polymer surface and cooling medium assumes finite values. In ref. [4], the heat transfer coefficient (h) was determined for a system of iPP plates quenched in water at a level of 350 W/(Km^2). The influence of the thermal resistance at the boundaries is best characterized by the so-called Biot number, defined for a plate as $0.5hd/K$. In the case of thick plates, 10 mm and thicker, such as those studied in this article, the Biot number assumes a value above 10. According to ref. [18], such large value of the Biot number leads to a minor temperature increase for a thick plate. Threfore, at first approximation, we neglected thermal resistance at the boundary.

In general, both K and a depend on temperature, and they also change due to phase conversion. The effect of crystallization on K and a of iPP was discussed in ref. [1] on the basis of the experimental data presented in refs. [19] and [20]. In ref. [4], it was demonstrated that accounting for the changes in K and a in the modeling of heat transport and crystallization in quenched slabs of iPP had a little influence on obtained results. Hence, the values of a and K were assumed to be equal to those of the polymer melt: 9.5×10^{-8} m^2/s and 0.17 W m^{-1} K^{-1}.[21,22] The constant coefficients in eq. (1) allow one to solve this equation, with the assumption that the temperature function (T) is a sum of two components: T_1 and T_2,[18] which fulfill the following equations:

$$\frac{\delta^2 T_1}{\delta x^2} - a^{-1}\frac{\delta T_1}{\delta t} = 0 \quad (2)$$

with the initial and boundary conditions $T_1(0,x) = T_0$ and $T_1(t,0) = T_1(t,d) = T_e$, respectively, and

$$\frac{\delta^2 T_2}{\delta x^2} - a^{-1}\frac{\delta T_2}{\delta t} = K^{-1}A(x,t) \quad (3)$$

with the initial and boundary conditions $T_2(0,t) = 0$ and $T_2(t,0) = T_2(t,d) = 0$, respectively.

T_1 is the temperature during the cooling of the plate from T_0 to T_e without heat generation due to crystallization, whereas T_2 describes the temperature increase due to heat generation alone.

According to ref [18], the functions T_1 and T_2 have the forms:

$$T_1(x,t) = T_e + 4(T_0 - T_e)\pi^{-1}\sum_{n=0}^{\infty}(2n+1)^{-1}\sin[(2n+1)\pi x/d]\exp\{-at[(2n+1)\pi/d]^2\} \quad (4)$$

$$T_2(x,t) = 2a(Kd)^{-1}\sum_{n=1}^{\infty}\sin(n\pi x/d)\int_0^t\int_0^d \sin(n\pi x'/d) \times A(x',\tau)\exp\{-a(n\pi/d)^2(t-\tau)\}dx'd\tau \quad (5)$$

In the case of a rod and a pipe of a length much larger than the radius, the heat conduction equation in cylindrical coordinates is solved. Similarly, as in the case of a plate, it is assumed that the considered body is initially at a constant temperature (T_0), and the temperature of the outer surface is suddenly changed and kept further at a constant level (T_e). Hence, the boundary condition for the heat transport problem in a rod of radius R is $T(t,R) = T_e$. The cooling of the inner pipe surface by air inside the pipe is neglected due to the low heat capacity of air, and hence, a zero heat flow through the inner surface is assumed. Therefore, the boundary conditions are $T(t,R_b) = T_e$ and, at $r = R_a$, $K[\delta T(t,r)/\delta r] = 0$, where r is the radial coordinate and R_a and R_b denote the inner and outer radii of a pipe, respectively. Similarly, as in the case of a plate, the functions describing separately the temperature distributions inside the material due to cooling and due to heat generation have to be found. The T_1 function for the rod is in the following form:[18].

$$T_1(r,t) = T_e + 2R^{-1}(T_0 - T_e)\sum_{n=1}^{\infty}J_0(r\alpha_n) \times [J_1(R\alpha_n)\alpha_n]^{-1}\exp(-a\alpha_n^2 t) \quad (6)$$

where r is the radius ($r < R$), J_0 and J_1 are the Bessel functions, and α_n are the positive roots of $J_0(R\alpha) = 0$.

For the pipe T_1 is in the form:

$$T_1(r,t) = T_e + (T_0 - T_e)\pi\sum_{n=1}^{\infty}\exp(-a\alpha_n^2 t)D(r)(J - J^{-1})^{-1} \quad (7)$$

where $J = J_1(R_a\alpha_n)/J_0(R_b\alpha_n)$ and $D(r) = J_0(r\alpha_n)Y_1(R_a\alpha_n) - Y_0(r\alpha_n)J_1(R_a\alpha_n)$, and α_n are the positive roots of $J_0(R_b\alpha_n)Y_1(R_a\alpha_n) - Y_0(R_b\alpha_n)J_1(R_a\alpha_n) = 0$, Y_0 and Y_1 are the Bessel functions, and r denotes the radius: $R_a < r < R_b$.

The T_2 functions are obtained by multiplication of the solutions of the heat conduction equation for the instantaneous cylindrical heat sources of unit strength in the rod and the hollow cylinder, respectively, by $2\pi A(r',\tau)aK^{-1}$ and integration over the ranges $0 < \tau < t$ and $0 < r' < R$ for the rod and $R_a < r' < R_b$ for the pipe. Hence, for the rod

$$T_2(r,t) = 2aK^{-1}R^{-2}\sum_{n=1}^{\infty}J_0(r\alpha_n)J_1(R\alpha_n)^{-2}\int_0^R J_0(r'\alpha_n) \times r'\int_0^t A(r',\tau)\exp[-a\alpha_n^2(t-\tau)]\,d\tau\,dr' \quad (8)$$

and for the pipe

$$T_2(r,t) = 0.5\pi^2 aK^{-1}\sum_{n=1}^{\infty}\alpha_n^2(J^2-1)^{-1}D \times (r)\int_{R_a}^{R_b}D(r')r'\int_0^t A(r',\tau)\exp[-a\alpha_n^2(t-\tau)]\,d\tau\,dr' \quad (9)$$

Heat release during crystallization in polymer bulk samples can be approximated with bulk heat generation function in the form:

$$A = \Delta L\frac{d\alpha(t)}{dt} \quad (10)$$

where ΔL is the heat released during crystallization of polymer volume unit and α(t) denotes the local, momentary conversion degree of melt into spherulites, which is determined by nucleation and spherulite growth rate. Although the heat of crystallization and the spherulite growth rate depend on temperature, the polymer nucleation also depends on thermal history.

EXPERIMENTAL

To collect the data necessary for modeling the crystallization of iPP, Malen P F401 (Orlen S.A, Plock, Poland), with a melt flow index of 2.5 g/10 min, was studied. The growth rate of F401 iPP spherulites in thin films was measured in the temperature range 124–145°C during isothermal crystallization conducted on a Linkam (Waterfield, UK) hot stage mounted in a light microscope. The DSC (Du Pont, Wilmington, DE, TA 2000) measurements were carried on iPP samples to determine heat of crystallization and crystallization kinetics during cooling. The samples were heated up to 220°C, melt annealed for 3 min, and cooled down at various rates. For more efficient cooling, the standard DSC cover was replaced by another, specially designed cap. It was composed of a thermally insulated aluminum element with the shape of the letter *H*. Liquid N_2 was poured into the upper cup of the letter *H*, whereas the lower cup covered both the sample and the DSC furnace. The DSC apparatus was able to maintain control over a cooling rate up to 40 K/min. For faster cooling, a quenching experiment was performed, during which the maximum level of LN_2 was kept in an aluminum cup and the DSC heater was inactive. The average cooling rate until the onset of crystallization was 150 K/min.

For comparison with the theoretical predictions, the decrease of temperature in iPP plates during cooling was measured. A wide iPP plate was obtained by compression molding in a rectangular metal mold 12 mm thick. The chromega–constantan thermocouple made of wires with a diameter of 0.127 mm was embedded in the plate in equal distances from both plate surfaces. The plate surrounded by the mold, wrapped in a thin aluminum foil, was heated in a press to 220°C, kept for several minutes at this temperature, and rapidly submerged in water bath at room temperature. When the ambient temperature was reached inside the plate, the plate was heated again to 120°C and quenched in the water bath. During cooling, the temperature inside the plate was measured. The water was agitated to improve the heat transfer. The thickness of the plate measured in the central part containing the thermocouple was only about 10.4 mm because of a nonuniform volume contraction due to crystallization

MODELING OF CRYSTALLIZATION

The temperature dependencies of the spherulite growth rate ($g(T)$) of iPP is well known:[23]

$$g(T) = g_0 \exp\{-U[R(T - T_\infty)]^{-1}\} \times \exp\{-K_g[T(T_m^0 - T)]^{-1}\} \quad (11)$$

where U = 1500 cal/mol, T_∞ = 231.2 K, T_m^0 = *458.2 K*, and T is the crystallization temperature, whereas g_0 and K_g depend on the regime of crystallization for a given iPP. On the basis of the plot $\ln g + U[R(T - T_\infty)]^{-1}$ versus $T^{-1}(T_m^0 - T)^{-1}$, K_g and g_0 were found to be 3.18×10^5 K^2 and 1945 cm/s in Regime III and 1.9×10^5 K^2 and 3.40 cm/s in Regime II of crystallization, respectively. The temperature of the transition from Regime II to Regime III was determined as 137°C.

From the DSC measurements, it was found that the amount of heat released during crystallization as a function of crystallization peak temperature, T, could be approximated in the following way:

$$\Delta L_w(\mathrm{J/g}) = 0.1696\, T\,(^\circ\mathrm{C}) + 78.55 \quad \text{for} \quad T > 103.12^\circ\mathrm{C} \quad (12a)$$

$$\Delta L_w(\mathrm{J/g}) = 3.497\, T\,(^\circ\mathrm{C}) - 264.67 \quad \text{for} \quad T < 103.12^\circ\mathrm{C} \quad (12b)$$

we calculated ΔL from ΔL_w, assuming a heat of fusion value of 209 J/g,[24] a crystalline phase density of 0.946g cm^{-3}, and an amorphous phase density of 0.854 g/cm^3.

To find the parameters describing the conversion rate at various cooling rates, we fitted the theoretically predicted curves to the DSC data, employing the procedure described next. First, an instantaneous primary nucleation was assumed, which was justified by the heterogeneous character of primary nucleation in iPP in the considered temperature range.[25] Therefore, the conversion degree during cooling could be described by the formula.[1,26]

$$\alpha(\tau) = 1 - \exp\left\{-(4/3)\pi D\left[\int_0^\tau G(\tau')\, d\tau'\right]^3\right\} \quad (13a)$$

where spherulite growth rate (G) is a function of time passed from the beginning of crystallization.

Substituting the temperature, $T(\tau)$, for the time, one obtains

$$\alpha^*(T) = 1 - \exp\left\{-(4/3)\pi D v^{-3}\left[\int_T^{T_s} g(T')\, dT'\right]^3\right\} \quad (13b)$$

where T_s denotes the temperature of the beginning of crystallization and v is the cooling rate. By fitting the series of curves described by eqs. (11) and (13b) to DSC data, we determined D and T_s as dependent on v (K/min):

$$T_s\,(^\circ\mathrm{C}) = 129.171\exp(-0.001214v) \quad (14)$$

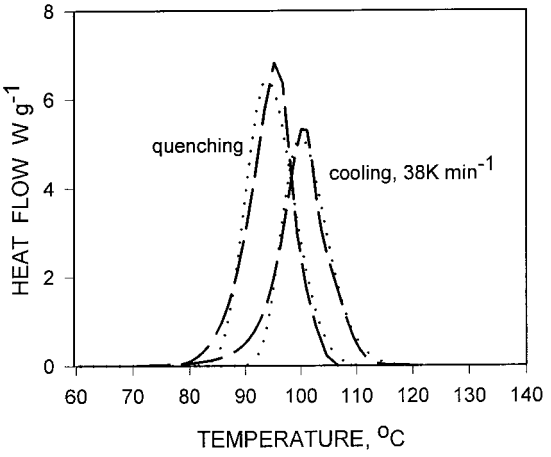

Figure 1 Comparison of DSC curves recorded during the cooling of iPP samples at a rate of 38 K/min and during quenching (dashed lines) with the theoretically predicted curves (dotted lines).

$$D\ (\mathrm{cm}^{-3}) = (3.6 \times 10^4)\exp(0.063v) \quad \text{for} \quad v < 38\ \mathrm{K/min} \quad (15a)$$

$$D\ (\mathrm{cm}^{-3}) = (3.16 \times 10^5)\exp(0.0062v) \quad \text{for} \quad v > 38\ \mathrm{K/min} \quad (15b)$$

Equations (12b) and (15b) are based on the quenching experiment. Independently, it was found that the same eq. (14) described T_s well in both cases, during controlled cooling and during quenching. The exemplary DSC curves recorded experimentally and the respective curves calculated based on eqs. (11) and (13b) are shown in Figure 1. A reasonable fit was achieved except for the very end of crystallization.

The local conversion of melt into spherulites can be accelerated by the temperature gradient due to the contribution of spherulites nucleated in the colder region of a material.[13,16] This effect depends, however, on the temperature, temperature gradient, and nucleation intensity. It was estimated in ref. [16] that a temperature difference greater than several degrees per distance equal to the average spherulite radius is required for the acceleration of the conversion. From preliminary calculations of the temperature distribution inside the considered objects during cooling, it followed that high temperature gradients of an order of 50–100 K/mm could be expected only in their outer parts, which were cooled very fast. The polymer there solidified at large supercoolings, where primary nucleation might have been too dense for the acceleration of the conversion rate due to the temperature gradient. The equation for the conversion degree during crystallization in bulk in the constant temperature gradient derived in ref. [16] allowed us to estimate the effect of the temperature gradient for a given cooling rate. T_s and D were estimated from eqs. (14) and (15), and the conversion–time dependence was calculated for a local temperature equal to T_s. The expected temperature gradient had little influence on the conversion rate; for T_s and D as calculated for $v = 60$ K/min, the gradient of 50 K/mm did not speed up the conversion, whereas a gradient of 100 K/mm had only a weak effect. Therefore, in the subsequent modeling of solidification in pipes, rods, and plates, the conversion rate and conversion degree were treated as dependent on the local temperature and thermal history only and not on the temperature gradient.

In the modeling of the crystallization inside thick-walled products, the following procedure was applied: the temperature distribution across the polymer in subsequent time intervals (1–3 s) was calculated according to eqs. (4)–(9), depending on the shape of the considered object. The average local cooling rates were computed, which permitted us to evaluate the values of T_s and D on the basis of eqs. (14) and (15). Below T_s, the conversion rate and heat generation rate, according to eqs. (13b) and (10), respectively, were calculated, where g and ΔL values were determined by local momentary temperature [eqs. (11) and (12)]. The calculations were carried out until the T_e temperature was reached inside the entire considered object. The temperature distributions during cooling, with crystallization neglected, were also computed. The calculations were also conducted for the cooling of plate surfaces at a constant rate.

COMPARISON OF THE THEORETICAL PREDICTION WITH THE EXPERIMENTAL MEASUREMENTS OF TEMPERATURE DECAY INSIDE IPP PLATES

The temperature decrease in the center of the 10.4 mm thick iPP plate was calculated for cooling from 220°C and from 120°C to room temperature according to the procedure described in the previous sections. For cooling from 220°C, we accounted for the crystallization of iPP. In addition, the cooling curve for the 12 mm thick plate was also computed. The comparison of experimental results and calculations is shown in Figure 2.

During the cooling of an iPP plate from 120°C, the temperature decreased continuously with time, whereas during cooling from 220°C, after an initial drop, a slight increase of the temperature was observed around 115°C due to crystallization. Then, the temperature fell again. For cooling from 120°C, a good agreement between the theoretically calculated curve and the experimental data was achieved. However, for cooling from 220°C, the temperature drop inside the plate was initially slower than that predicted theoretically for the plate thickness of 10.4 mm. The experimental data approached and then followed the respective curve after the first 3 min, that is, after the onset of the temperature increase due to crystallization. The

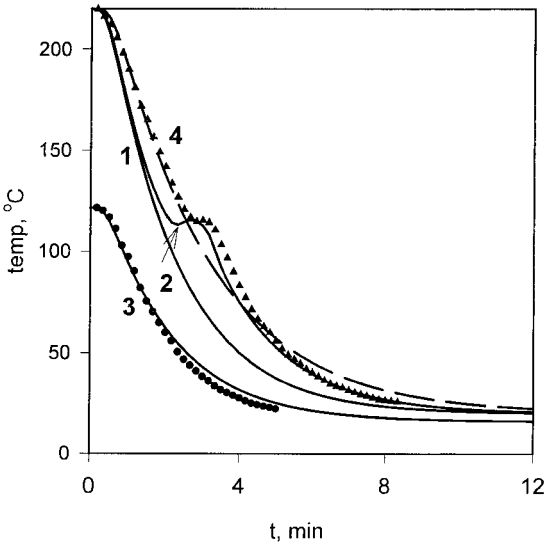

Figure 2 Temperature decrease inside the iPP (Malen P F401) plate measured (symbols) and calculated (lines) for a plate of thickness 10.4 mm for (1) cooling from 220°C with crystallization neglected, (2) cooling from 220°C with crystallization accounted for, (3) cooling from 120°C, and (4) also for a plate of thickness 12 mm for cooling from 220°C with crystallization neglected.

initial temperature fall measured inside the iPP plate followed more closely the cooling curve calculated for the plate thickness of 12 mm. Therefore, we concluded that the deviation of experimental data from the theoretically predicted curve was related primarily to the initial larger thickness and volume shrinkage of the polymer due to crystallization. The discrepancies could have also resulted in part from nonuniformity of sample thickness and neglect of the heat transfer condition at the polymer boundary. The possible effect of the latter would diminish with an increase in thickness of the considered plates.

Nevertheless, the theoretical model demonstrated in the previous sections proved to be useful for the predictions of the temperature drop inside a polymer crystallizing during cooling; hence, it was applied to predict the temperature during cooling of plates, pipes, and rods made of iPP.

RESULTS OF MODELING

The computations were carried out for T_0 = 220°C and T_e = 20°C and also for T_0 = 180°C and T_e = 0°C. The following objects were considered: rods of radii 10, 20, and 40 mm; plates 20 and 40 mm thick; and pipes having inner and outer radii, R_a and R_b of 50 and 60, 50 and 70, and also 100 and 140 mm, respectively. The results obtained for pipes were similar to those obtained for plates twice as thick as pipes due to small R_b/R_a ratios.

Exemplary time dependencies of the temperature inside pipes obtained with and without accounting for the polymer crystallization are demonstrated in Figures 3 and 4. The curves show the temperature at various positions across the pipe wall spaced by 0.2 of wall thickness. The crystallization significantly influenced the temperature inside a polymer during cooling, whereas the temperature near the outer surface of a pipe was only affected little. With the increase in the distance from the outer surface, the influence on the crystallization process became more pronounced. The temperature near the inner surface of a pipe elevated after an initial drop and started to decrease again when the crystallization was completed. The effect of crystallization on the temperature became stronger with the increase in the thickness of pipe wall. In Figure 5, the conversion degree against time at selected positions across the pipe wall is plotted. The polymer solidified very fast near the outer surface of a pipe, but near the inner surface, the crystallization started much later, and it was completed after a relatively long time passed from the beginning of cooling. When the polymer began to crystallize near the inner pipe surface, the temperature of the outer layers was already low, although it slightly increased due to the heat flow from the interior.

In Figure 6, the temperature at various positions across the pipe wall is plotted against the conversion

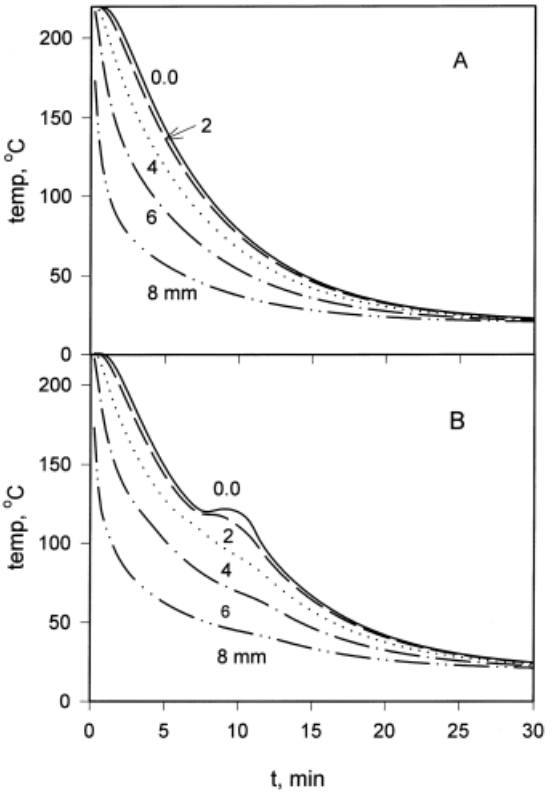

Figure 3 Time dependencies of the temperature inside an iPP pipe with R_a = 50 mm and R_b = 60 mm during cooling from 220 to 20°C across the pipe wall: (A) crystallization not accounted for and (B) crystallization accounted for. Numbers denote distances from the inner pipe surface.

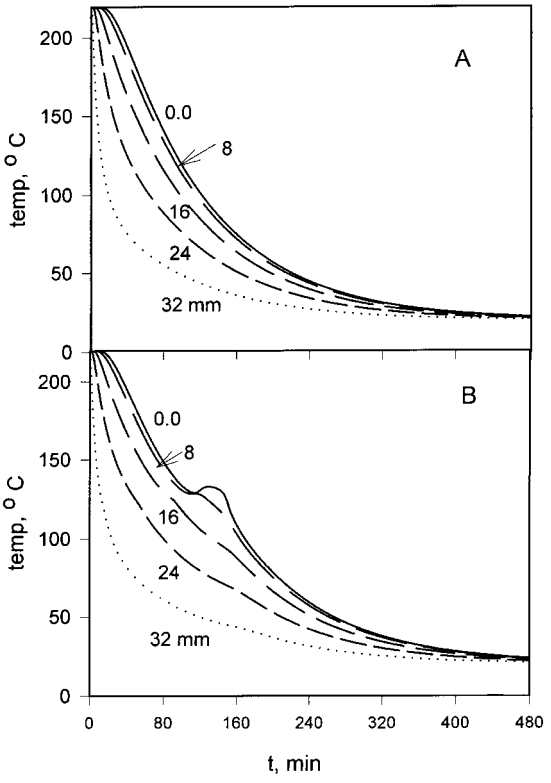

Figure 4 Time dependencies of the temperature inside the iPP pipe with R_a = 100 mm and R_b = 140 mm during cooling from 220 to 20°C across the pipe wall: (A) crystallization not accounted for and (B) crystallization accounted for. Numbers denote distances from the inner pipe surface.

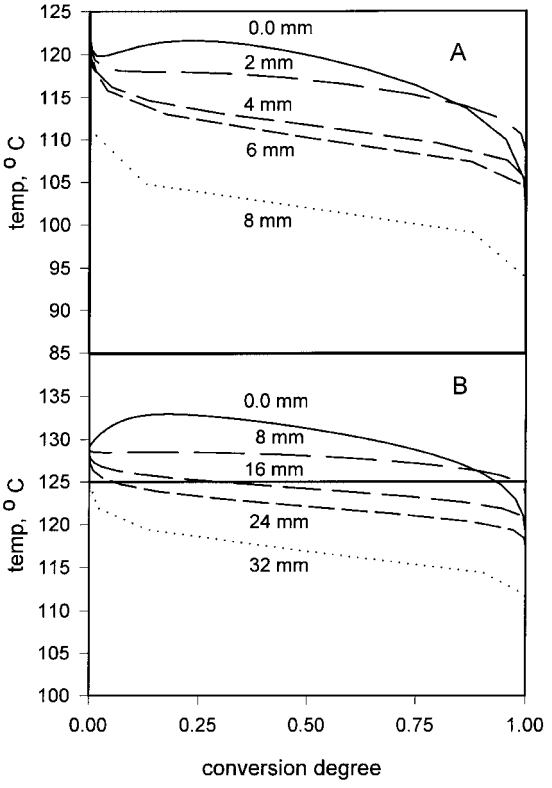

Figure 6 Temperature against conversion degree inside the iPP pipes during cooling from 220 to 20°C across the pipe wall: (A) R_a = 40 mm and R_b = 50 mm and (B) R_a = 100 mm and R_b = 140 mm. Numbers denote distances from the inner pipe surface.

degree. Comparison of Figure 6(a) and 6(b) illustrates the influence of the thickness of the pipe wall on the temperature of polymer solidification. With the increase in wall thickness from 10 to 40 mm, the temperature of solidification of the internal pipe region increased by 20 K. Hence, in the pipe having a wall 40 mm thick, most of iPP material crystallized above 125°C.

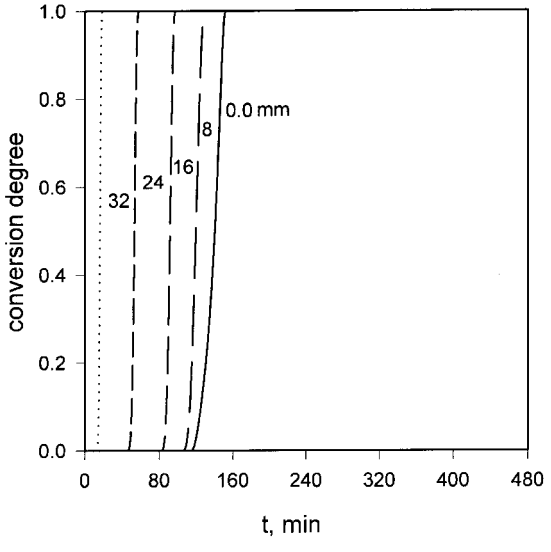

Figure 5 Time dependencies of the conversion degree inside the iPP pipe with R_a = 100 mm and R_b = 140 mm during cooling from 220 to 20°C across the pipe wall. Numbers denote distances from the inner pipe surface.

The results obtained for the rods plotted in Figures 7–10 exhibited similar tendencies. The temperature inside the polymer was greatly influenced by the rod radius. The temperature decreased inside the rod faster than in the pipe with wall thickness equal to the rod radius, so the polymer crystallized earlier and at a lower temperature. The temperature in the outer region did not increase when the rod's interior crystallized. The elevation of polymer crystallization temperature inside the thicker rod was even stronger than in the pipe.

Calculations for cooling the pipe with a 20 mm thick wall from 180 to 20°C and from 220 to 0°C were also performed to estimate of the possible influence of the initial and end temperatures. The decrease of T_0 to 180°C had a very little effect on both the crystallization and the temperature in the pipe interior, although the cooling time was decreased. A faster temperature drop during crystallization was observed due to the decrease of T_e to 0°C.

The cooling of the external pipe surfaces at a constant rate was also considered and found ineffective. A cooling rate around 100 Kmin was required to accelerate the cooling of the interior of the 20 mm thick plate. However, the temperature gradient across the

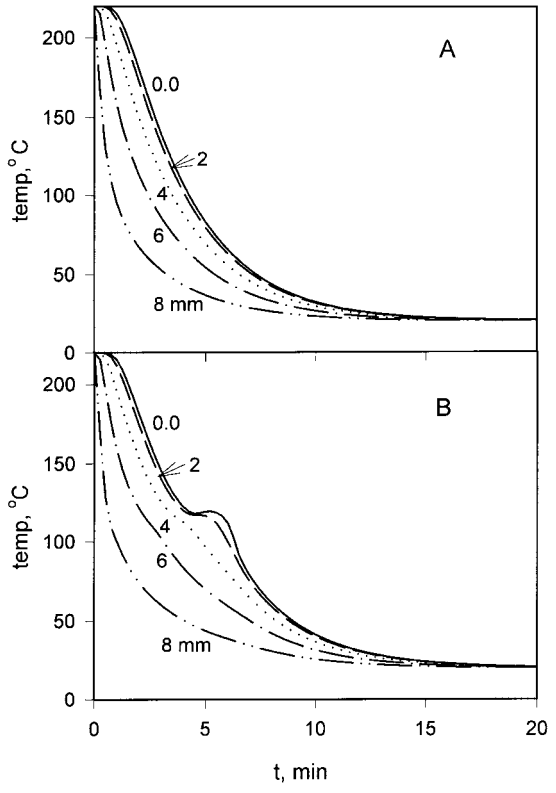

Figure 7 Time dependencies of temperature inside the iPP rod with $R = 10$ mm during cooling from 220 to 20°C along the rod radius: (A) crystallization not accounted for and (B) crystallization accounted for. Numbers denote distances from the rod center.

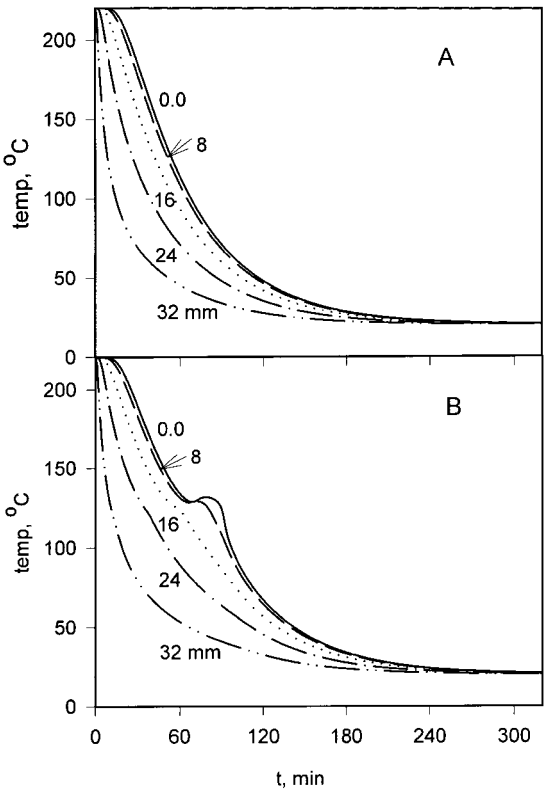

Figure 8 Time dependencies of temperature inside the iPP rod with $R = 40$ mm during cooling from 220 to 20°C along the rod radius: (A) crystallization not accounted for and (B) crystallization accounted for. Numbers denote distances from the rod center.

plate was so high that when the outer region reached ambient temperature, the temperature in the interior still exceeded 150°C. Therefore, the cooling of the outer region to a very low temperature would be necessary in industrial conditions. In the latter case, a different form of the T_1 function, appropriate for the respective boundary condition, was used.[18]

DISCUSSION

The proposed procedure of modeling of the temperature field and the polymer crystallization allowed us to consider objects of different geometries: plates, pipes, and rods. The temperature decline measured experimentally inside the iPP plate confirmed the usefulness of the proposed model for the prediction of the temperature change during cooling of thick-walled objects from the molten state. Although neglecting the heat transfer resistance at the polymer boundary limits the modeling to thick-walled products efficiently cooled during solidification, the possible modification of the boundary conditions of heat conduction equation will allow wider application of the demonstrated approach.

The modeling of heat transport inside plates, pipes, and rods showed that the crystallization of a polymer results in a significant temperature increase in the polymer. The crystallization in the interior causes the temperature elevation, whereas in outer regions, the crystallization only slows down the cooling. Nevertheless, neglecting crystallization in estimation of the

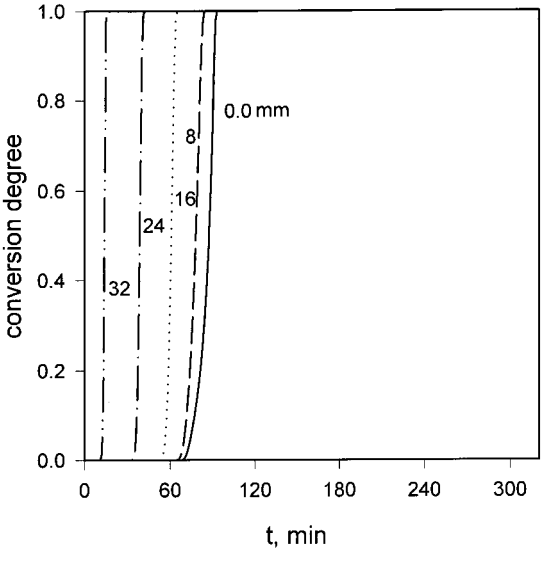

Figure 9 Time dependencies of conversion degree inside the iPP rod with $R = 40$ mm during cooling from 220 to 20°C along the rod radius Numbers denote distances from the rod center.

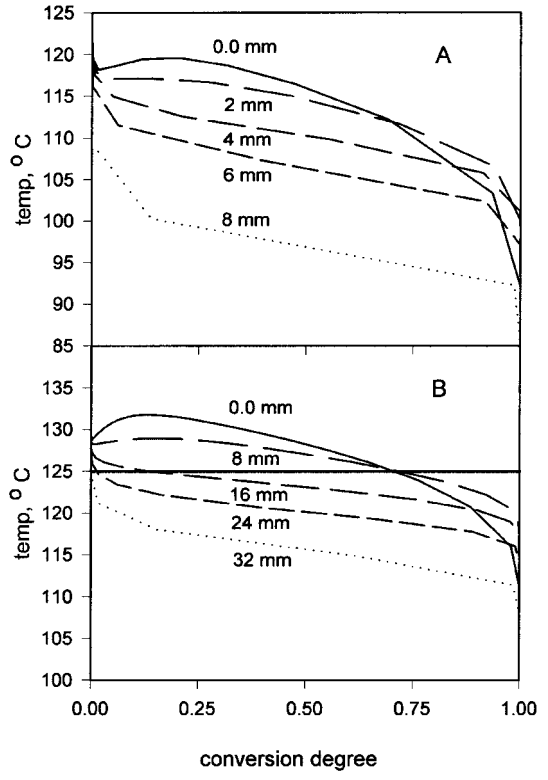

Figure 10 Temperature against conversion degree inside the iPP rods during cooling from 220 to 20°C along the rod radius: (A) $R = 10$ mm and (B) $R = 40$ mm. Numbers denote distances from the rod center.

temperature inside thick-walled products leads to unrealistic results.

The crystallization temperature is crucial to the polymer properties. It is known that the elevation of crystallization temperature leads to phenomena unfavorable for polymer strength: the ties between lamellae bonding between the crystalline and amorphous phases are worse, average spherulite size increases, and fractionation causes the exuding of the low-molecular-weight fraction to spherulitic boundaries.

The temperature during polymer solidification inside bulky products depends on the thickness of their walls. An increase in the thickness leads to a markedly higher crystallization temperature. Because the increase in the temperature of polymer crystallization is unavoidable, the proper molecular characteristics of the polymer are important. The crystallization inside thick-walled products is delayed compared to the solidification of the outer regions. It is, therefore, important to ensure good heat subtraction during a time longer than necessary for solidification of the outer regions. The time required for completion of crystallization inside the polymer could be as long as 90 min for a rod having a 40-mm radius and 160 min for a pipe with a wall 40 mm thick.

APPENDIX: COMMENT ON KOLMOGOROFF ARTICLE ON OVERALL CRYSTALLIZATION KINETICS[10]

The basic reasoning of Kolmogoroff started from the estimation of the probability of one nucleation event in the volume V' during the time interval $\Delta t'$: the probability of one event was expressed by Kolmogoroff as

$$f(t')V'\Delta t' + o(\Delta t') \tag{A.1}$$

where f denotes the nucleation rate and $o(\Delta t')$ is an infinitely small quantity as compared with $\Delta t'$. The probability of nucleation of more than one event in the volume equals $o(\Delta t')$ (an infinitely small quantity). The arbitrary point P belongs at time t to that portion of the sample that is occluded by a growing domain if its center is nucleated at time $t' < t$ and within a distance from the point P given by the formula $c(n)\int_{t'}^{t} G(\tau)d\tau$, where G is the growth rate, n denotes the direction, and c is the dependence of the growth rate on the direction (for isotropic growth, $c = 1$). According to Kolmogoroff, the probability equals $f(t')\ V'(t')\ \Delta t' + o(\Delta t')$, where $V'(t') = (4\pi/3)c^3[\int_{t'}^{t} G(\tau)\ d\tau]^3$. The probability that point P remains unoccluded by domains nucleated at t' is $1 - f(t')\ V'(t')\ \Delta t' + o(\Delta t')$. Point P remains unoccupied at time t if it is outside domains nucleated in subsequent time intervals $\Delta t_i'\ i = 1 \ldots n$ until time t ($n = t/\Delta t'$). Hence, the probability of this event is the product

$$q = \prod_{i=1}^{n} [1 - f(t_i')V'(t_i')\Delta t_i'] + o(1) \tag{A.2a}$$

Because $\Delta t'$ is infinitely small, Kolmogoroff transformed eq. (A.2a) to

$$\ln q = -\sum_{i=1}^{n} f(t_i')V'(t_i')\ \Delta t_i' + o(1) = -\int_0^t f(t')V'(t')dt' \tag{A.2b}$$

We now know that the correct expressions for the probabilities of m events in the volume V' during time interval $\Delta t'$ should be calculated according to the Poisson distribution:

$$P_m = \exp[-f(t')V'\Delta t'][f(t')V'\Delta t']^m/m! \tag{A.3}$$

Therefore, the probability, Q, that point P remains unclouded at time t is

$$Q = \prod_{i=1}^{n} \exp[-\alpha(t_i')V'(t_i')\Delta t_i'] \tag{A.4a}$$

$$Q = \exp\left[-\sum_{i=1}^{n} f(t_i')V'(t_i')\Delta t_i'\right] = \exp\left[-\int_0^t f(t')V(t')dt\right]$$

$$= \exp(-y) = \sum_{k=0}^{\infty} (-1)^k y^y (k!)^{-1} \quad \text{(A.4b)}$$

Equation (A.2a), in the form used by Kolmogoroff, can be obtained from eq. (A.4a) by expanding the right hand side in series and neglecting all components containing the powers of Δt higher than 1. However, this requires an inconsistency in the treatment because in eq. (A.2a), the terms containing the products' time intervals, for example, $\Delta t_i' \, \Delta t_i' \, \Delta t_k'$ $i \neq j \neq k$, are not neglected, although they are small.

The inaccurate eq. (A.2a) is a result of Kolmogoroff neglecting the probability of the occlusion of a sampling point by more than one domain nucleated in $\Delta t'$ that is, Kolmogoroff neglected impingement of domains nucleated in the same time intervals. Although the error due to simplification, $1 - f(t')V'(t')\Delta t'$ instead of the exact term, $\exp[-f(t')V'(t')\Delta t']$, can be negligible, the multiplication of these probabilities as in eq. (A.2a) enhances the error. Next, we show the exact expression for q as derived by Kolomogoroff in eq. (A.2a). Introducing the notation $x_i = f(t_i')\, V(t_i')\, \Delta t_i'$ and performing the multiplication, we obtain

$$\prod_{i=1}^{n} (1 - x_i) = 1 - \sum_{i=1}^{n} x_i + \sum_{i=1}^{n-1} x_i \sum_{j=i+1}^{n} x_j$$

$$- \sum_{i=1}^{n-2} x_i \sum_{j=i+1}^{n-1} x_j \sum_{l=j+1}^{n} x_l + \cdots + (-1)^k \sum_{i=1}^{n-k+1} x_i \sum_{j=i+1}^{n-k+2}$$

$$x_j \cdots \sum_{m=p+1}^{n} x_m \cdots + (-1)^n x_1 x_2 \cdots x_n \quad \text{(A.5)}$$

In eq. (A.5), for $\Delta t_i' \to 0$, $\sum_{i=1}^{n} x_i$ can be expressed as $y = \int_0^t f(t')V'(t')\, dt'$.

For the other components of eq. (A.5), we can write

$$\sum_{i=1}^{n-k+1} x_i \sum_{j=i+1}^{n-k+2} x_j \cdots \sum_{m=p+1}^{n} x_m$$

$$= \left[\sum_{i=1}^{n} x_i \sum_{j=1}^{n} x_j \cdots \sum_{m=1}^{n} x_m\right](k!)^{-1} - H_k \quad \text{(A.6)}$$

$[\sum_{i=1}^{n} x_i \sum_{j=1}^{n} x_j \cdots \sum_{m=1}^{n} x_m](k!)^{-1}$ converges to $y^k/k!$, where H_k is a sum of certain products of x_i, which are lacking in eq. (A.2a). The last term in eq. (A.5) equals $x_1 x_2 x_3 \ldots x_n$ instead of $y^n/n!$. Hence, eq. (A.5) is now

$$q = 1 - y + \sum_{k=2}^{n} (-1)^k (y^k/k! - H_k) \quad \text{(A.7)}$$

If the terms H_k is neglected in eq. (A.7), only the term $1 - y$ is accurate, and the higher the power of y is the larger the error is.

Kolmogoroff introduced the error by neglecting in eq. (A.1) events of more than one nucleation in the volume V in the time interval Δt. The additional terms, H_k, appeared in the expression for the probability q [see eq. (A.7)] due to this error. In the subsequent operations, the terms H_k were erroneously neglected. The two errors canceled themselves, and accidentally, a correct final formula was obtained by Kolomogoroff.

The erroneousness of Kolmogoroff's approach is best seen when it is applied to the instantaneous nucleation: on the right hand of eq. (A.5), all terms are equal to zero except for the two first because only x_1 is nonzero. In this case, H_k converges to $y^k/k!$ The expression for the probability that point P remains unoccluded at time t will then be $1 - V'D$, which is obviously erratic except for at the very beginning of crystallization.

References

1. Piorkowska, E. J Appl Polym Sci 1997, 66, 1015.
2. Plummer, C. J. G.; Kaush H. H. Colloid Polym Sci 1995, 273, 719.
3. Isayev, A. I.; Catignani, B. F. Polym Eng Sci 1997, 37, 1526.
4. Carvalho de, B.; Bretas, R. E.; Isayev, A. I. J Appl Polym Sci 1999, 73, 2003.
5. Koppelmann, J.; Fleischmann, E.; Leitner, G. Rheol Acta 1987, 26, 548.
6. Janeschitz-Kriegl, H.; Fleischmann, E.; Geymayer, W. In Polypropylene; Karger-Kocsis, J., Ed.; Chapman and Hall: London, 1994; p 295.
7. Sombatsompop, N.; Chonnyom, D.; Wood, A. K. J Appl Polym Sci 1999, 74, 3268.
8. Evans, U. R. Trans Faraday Soc 1945, 41, 365.
9. Avrami, M. J Chem Phys 1939, 7,1103; 1940, 8, 212; 1941, 9, 177.
10. Kolmogoroff, A. N.; Isvestia Akad Nauk 1937, 3, 355.
11. Eder, E. In Crystallizing Polymers in Macromolecular Design of Polymeric Materials; Hatada, K.; Kitayama, T.; Vogl, O., Eds.; Marcel Dekker: New York, 1997; p 761.
12. Lovinger, A. J.; Chua, J. O.; Gryte C. C. J Polym Sci Part B: Polym Phys 1977, 15, 641.
13. Pawlak, A.; Piorkowska, E. Colloid Polym Sci 2001, 279, 939.
14. Swiminarayan, S.; Charbon, C. Polym Eng Sci 1998, 38, 634.
15. Charbon, C.; Swiminarayan, S. Polym Eng Sci 1998, 38, 644.
16. Piorkowska, E. J Appl Polym Sci 2002, 86, 1351.
17. Nakamura, K.; Katayama, K.; Amano, T. J Appl Polym Sci 1973, 17, 1031.
18. Carslaw, H. S.; Jaeger, J. C. Conduction of Heat in Solids; Clarendon: Oxford, England, 1959.
19. Eiermann, K. Kolloid Z 1964, 201, 3.
20. Eiermann, K. J Polym Sci Part C Polym Symp 1964, 6, 157.
21. Fuller, T. R.; Fricke, A. L. J Appl Polym Sci 1971, 15, 1729.
22. Pattnaik, S.; Thompson, E. V. Polym Prepr (Am Chem Soc Div Polym Chem) 1981, 22, 199.
23. Clark, E.; Hoffman, D. Macromolecules 1984, 17, 878.
24. Wunderlich, B. Crystal Structure, Morphology, Defects; Macromolecular Physics, Vol. 1; Academic: New York, 1973; p 388.
25. Galeski, A. In Polypropylene, Karger-Kocsis, J., Ed.; Chapman and Hall: London, 1994; p 116.
26. Piorkowska, E. J Phys Chem 1995, 99, 14016.